ISSN 1846-6168 (Print), ISSN 1848-5588 (Online)
https://doi.org/10.31803/tg-20260518173334

Original scientific paper
Received: 2026-05-18, Accepted: 2026-06-23

Numerical Modeling of Hydrodynamic Vibrations in the Flow Passage of Centrifugal Pumps

Amir G. Mustafayev, Sanam J. Muslimov*

Abstract: The numerical modeling method enables researchers to study hydrodynamic processes through pump flow passage testing which serves as evidence to support modifications in existing centrifugal pump design methods. Hydrodynamic vibration critically impacts centrifugal pump reliability and performance under off-design conditions. This study presents a numerical model coupling rotor dynamics with hydraulic characteristics to analyze vibration's effect on flow rate and head. The approach integrates mechanical motion equations with vibration-dependent hydraulic loss models and harmonic-response solutions. We propose a physical mechanism where vibration arises from transit-inertial flow interactions in impeller passages, periodically disturbed by the volute tongue. The model predicts predominant vibration at blade-passing frequency, strongest transversely. Validation used vibration data from NM-type oil pipeline pumps at reduced flow. Results show flow rate departures increase hydrodynamic instability, elevating vibration and reducing hydraulic performance. This model enables vibration diagnostics and pump design optimization.

Keywords: centrifugal pumps; energy characteristics; fluid flow; hydrodynamic vibration; head and flow rate

1 INTRODUCTION

One of the most common types of hydrodynamic machines is the centrifugal pump.

During operation, these machines are subjected to a specific hydraulic regime accompanied by structural vibration. This complicates the operation of hydraulic machines, shortens the interval between repairs, and ultimately leads to undesirable failures.

Hydraulic machines are designed for specific operating parameters. One type of hydraulic machine is the centrifugal pump, which is designed on the basis of fluid capacity (flow rate) and the head developed by the pump.

The operating mode of centrifugal pumps is mainly governed by these two parameters. Although studying these parameters is associated with deviations in pump operation and with the minimization of energy losses during service, it also makes it possible to preserve pump components and prevent damage from vibration-induced hydraulic impacts.

Studies show that the higher the power of the pumping unit and the stronger the unsteady pulsations, the greater the flow disturbances in the pump flow passage. In this case, the resulting flows hinder fluid passage through the hydraulic machine, reduce pump capacity, and increase energy losses. During pulsation, the force and impact loads acting on the elements of the pump flow passage intensify significantly and transform into oscillatory motion. The consequences of vibration can be extremely destructive.

A high vibration level arises when pumps are operated outside their normal operating zone. Its negative effects may occur even during short-term operation under such conditions. If pumps are operated in these modes for a long time, the consequences of vibration may become severe and hazardous.

At present, at most oil pipeline transport facilities, due to the transition to a market economy, this situation has changed. However, the acute problem on existing trunk lines has not been eliminated, since they are oriented toward maximum oil supply to the market while not having exhausted their service life or while that service life is being successfully extended.

Hydrodynamic equipment must be operated, under the existing circumstances, together with the means of controlling its operating modes that were available at the time of commissioning.

This problem creates the need to search for methods and means that prevent or substantially reduce the vibration level of centrifugal pumps operating under reduced flow conditions.

The problem under consideration is relevant to all industries in which centrifugal pumps are used.

Under the current conditions, these methods and means impose constraints on the design of hydraulic machines. This is because, on the one hand, the phenomena under study occur either within these machines themselves, and on the other hand, the existing methods for controlling the operating modes of centrifugal pumps do not make it possible to influence these phenomena in the required directions. Throttling the flow at the station outlet and reducing the number of pumps connected in series only make it possible to reduce the volume of liquid passing through the pumps.

2 THEORETICAL PART

2.1 Differential Equations Describing the Dependence of Pump Flow Rate on Vibration

To assess the dependence of the flow rate Q on vibration in the vertical, transverse, and axial directions, a dynamic model of the following form is usually used:

$$Q = Q_0 - k_v A_v - k_t A_t - k_a A_a \quad (1)$$

Where, A_v, A_t, A_a - are the vibration amplitudes in the vertical, transverse, and axial directions, and k_v, k_t, k_a - are the coefficients describing the influence of vibration on the hydraulic efficiency of the pump.

Such a linear approach is based on rotor efficiency degradation models due to vibration proposed in the classical theory of centrifugal pumps and confirmed in rotor dynamics studies [1-5].

However, for accurate modeling, a system of differential equations is used:

$$m\ddot{x} + c\dot{x} + kx = F_{\text{hyd}}\left(Q, H\right) + F_{\text{unbalance}}, \quad (2)$$

where: $x(t)$ - the rotor displacement; c - the damping coefficient; k - the stiffness; F_{hyd} - the hydrodynamic force depending on flow rate and head; $F_{\text{unbalance}} = me\omega^2\sin(\omega t)$ - the force caused by imbalance [6, 7].

The hydrodynamic force is determined through a linear approximation of losses:

$$F_{\text{hyd}} = \alpha_1 Q + \alpha_2 H, \quad (3)$$

which is confirmed by studies on hydraulic transient processes [8, 9].

2.1.1 Differential Equations Describing the Dependence of Pump Head on Vibration

For centrifugal pumps, the head H under vibration is determined through a modified Euler equation [2, 10]:

$$H = H_0 - \beta_{\text{v}} A_{\text{v}}^2 - \beta_{\text{t}} A_{\text{t}}^2 - \beta_{\text{a}} A_{\text{a}}^2 \quad (4)$$

The quadratic effect of vibration is associated with losses of kinetic energy due to non-axial flow rotation and is confirmed in the theory of unstable processes [11, 12].

A more advanced model takes pressure dynamics into account:

$$\frac{\mathrm{d}H}{\mathrm{d}t} + aH = bQ - \gamma A(t), \quad (5)$$

where: $A(t)$ is the resultant vibration amplitude; the coefficients α, β, γ are determined from experimental ESP curves [13, 14].

After this, we write the dynamic flow-head-vibration model.

Combining (2), (3), (4), and (5), we obtain the system:

$$\begin{cases} m\ddot{x} + c\dot{x} + kx = \alpha_1 Q + \alpha_2 H + me\omega^2\sin(\omega t), \\ Q = Q_0 - k_{\text{v}} A_{\text{v}} - k_{\text{t}} A_{\text{t}} - k_{\text{a}} A_{\text{a}}, \\ H = H_0 - \beta_{\text{v}} A_{\text{v}}^2 - \beta_{\text{t}} A_{\text{t}}^2 - \beta_{\text{a}} A_{\text{a}}^2. \end{cases} \quad (6)$$

This system is used in ESP vibration models; see [15-17].

Studies show that, due to hydraulic losses and increased recirculation caused by vibration, the flow rate decreases linearly [1, 2, 4], while vibration disturbs the pressure distribution and the axial acceleration of the flow, causing the head to decrease quadratically [10, 11].

This ESP model is used in practice for failure diagnostics and for selecting operating modes [14, 15].

2.1.2 Basic Rotor Dynamics Model

For each spatial component (vertical, transverse, and axial), the motion of the rotor (pump assembly) can be described by the classical equation with external excitation forces:

$$m\ddot{x}(t) + c_x\dot{x}(t) + k_x x(t) = F_x(t) \quad (7)$$

$$m\ddot{y}(t) + c_y\dot{y}(t) + k_y y(t) = F_y(t) \quad (8)$$

$$m_z\ddot{z}(t) + c_z\dot{z}(t) + k_z z(t) = F_z(t) \quad (9)$$

Where: m - the effective mass (for transverse oscillations) or m_z is the axial mass; $c_{(\cdot)}$ - damping; $k_{(\cdot)}$ - the stiffness of the supports/system; $F_{(\cdot)}(t)$ - the external disturbing force set (rotor unbalance, hydrodynamic pulsations, gas action, impacts, contacts, etc.).

Katsuhiko Ogata's book (2010) presents a systematic theoretical study and exposition of methods for the analysis and synthesis of control systems. It develops mathematical models of dynamic systems and introduces optimal control. However, the book is strongly focused on linear systems; nonlinear methods are covered only to a limited extent, and less attention is given to modern, adaptive, and intelligent methods [18].

Typical components of $F(t)$:

Forced forces due to imbalance: $F_{\text{unb}}(t) = me\omega^2\cos(\omega t)$ (e - eccentricity; ω - rotational frequency), hydrodynamic forces depending on Q, H and operating mode:

$F_{\text{hyd}}(t) = f_{\text{hyd}}(Q, H, \dot{Q}, ...)$; random/noise disturbances F_{noise}.

2.1.3 Model of Vibration-Hydraulics Interaction

A pump is an interconnected hydrodynamic-mechanical system. To obtain the relationship between vibration amplitude and changes in Q and H, two groups of equations are usually used:

1) Hydraulic equations (pump state)

Classical static pump characteristic:

$$H = H_{\text{pump}}(Q, \omega) \text{ (for example, } H = H_0(\omega) - aQ^2) \quad (10)$$

But under vibration, hydrodynamic losses and inlet conditions change. A small-signal relationship can be written as:

$$\Delta H = G_{H,Q}\Delta Q + G_{H,x}x + G_{H,y}y + G_{H,z}z + ... \quad (11)$$

$$\Delta Q = G_{Q,H}\Delta H + G_{Q,x}x + G_{Q,y}y + G_{Q,z}z + ... \quad (12)$$

where $G_{H,x}$ is the sensitivity of head to displacement/vibration along x etc. These coefficients are obtained either from CFD/FSI calculations or empirically.

2) Coupled mechanics-hydraulics system

Substituting relations (11) and (12) into Eq. (2), we obtain coupled ODEs with feedback: mechanics excites the flow, and the flow changes the forces in the mechanical subsystem.

In simplified form:

$$m\ddot{x} + c_x\dot{x} + k_x x = me\omega^2\cos(\omega t) + \alpha_x Q(t) + \beta_x H(t) \quad (13)$$

and similarly for y, z, while $Q(t)$, and $H(t)$ are related through the pump characteristic and through the functions G.

2.2 Harmonic Analysis - Analytical Solution for a Stationary Forced Regime

If the excitation is harmonic (for example, imbalance at rotational frequency ω), and if the behavior can be considered linear in the vicinity of the operating point, then for one coordinate:

$$m\ddot{x} + c\dot{x} + kx = F_0\cos(\omega t) \tag{14}$$

The steady-state solution gives the amplitude:

$$X(\omega) = \frac{F_0}{m}\frac{1}{\sqrt{\left(\omega_n{}^2 - \omega^2\right)^2 + (2\zeta\omega_n\omega)^2}} \tag{15}$$

where $\omega_n = \sqrt{k/m}$ - the natural frequency, and $\zeta = c/(2m\omega_n)$ - the quality factor/damping.

Interpretation: at $\omega \to \omega_n$ (resonance) the amplitude grows; damping reduces the peak amplitude.

Relationship between vibration amplitude and changes in Q and H — models and solution examples

Practical engineering approach. Linear approximation

If experiments show that small changes in vibration lead to approximately linear changes in flow rate and head, one may assume:

$$Q(t) = Q_0 + \gamma_x x(t) + \gamma_y y(t) + \gamma_z z(t) \tag{16}$$

$$H(t) = H_0 + \eta_x x(t) + \eta_y y(t) + \eta_z z(t) \tag{17}$$

Here γ_i, η_i are empirical coefficients ($m^3/h\cdot mm^{-1}$ or $m\cdot mm^{-1}$), determined by regression from measurements.

Then the system (2) + (16), (17) can be solved numerically:

First $x(t)$, $y(t)$, and $z(t)$ must be found from (2) (knowing the Q, and H relationships), and then Q, and H are calculated using (16), and (17).

In the frequency domain, the amplitudes are substituted (16), and (17), and the change in the mean Q/H is obtained.

Nonlinear approximation for large amplitudes

If the effect is strong, a polynomial or logarithmic relationship is used:

$$Q = Q_0 + \sum_i \gamma_{1i}x_i + \sum_i \gamma_{2i}x_i^2 \ldots \tag{18}$$

or

$$H = H_0 \cdot \exp\left(-\sum_i k_i A_i\right) \tag{19}$$

where A_i is the vibration amplitude in direction i.

By solving the problem, we obtain the following analytical conclusions:

For the established harmonic response, using Eq. (15) for the vibration amplitudes and Eqs. (16) and (17), the change in the mean Q and H can be obtained:

For example:

$$\Delta Q = \gamma_x X + \gamma_y Y + \gamma_z Z \tag{20}$$

where X, Y, Z are the amplitudes of steady-state oscillations.

For the transient process in time: the solution of variant (2) with any $F(t)$ yields a transient part (terms $e^{-\zeta\omega nt}$) and a forced part. Numerically, it is solved by ODE-solvers (MATLAB, Python) and then substituted into (16), and (17).

For stability (resonance): when the mechanical natural frequency coincides with characteristic hydrodynamic frequencies, hydro-mechanical resonances are possible, in which even small excitation sharply reduces Q and H because of large vibration amplitudes. In the model this appears as a peak in $X(\omega)$ and then a significant ΔQ.

Let us consider a specific model example with imbalance and linear sensitivity.

For simplicity, let us write one coordinate in the transverse direction:

$$m\ddot{y} + c\dot{y} + ky = me\omega^2\cos(\omega t) + \beta Q(t) \tag{21}$$

$$Q(t) = Q_0 + \gamma_y y(t) \tag{22}$$

Substituting, we obtain a nonlinearly coupled ODE (linearized for small γ_y):

$$m\ddot{y} + c\dot{y} + (k - \beta\gamma_y)y = me\omega^2\cos(\omega t) + \beta Q_0 \tag{23}$$

It can be seen here that the hydraulic coupling changes the effective stiffness: $k_{\text{eff}} = k - \beta\gamma_y$. If $\beta\gamma_y$ is positive and close to k, the system may become less stable → vibration amplification and a drop in Q. The analytical solution is the amplitude according to (15) with k_{eff}.

The performed analyses show that, to solve the stated problem, it is advisable to use the following equations:

In mechanics: a second-order ODE (mass-damper - stiffness), Eqs. (7) – (9). Solution: analytical (harmonic) for a sinusoidal force (Eq. (15)) or numerical integration for a general $F(t)$.

In hydraulics: a static Q–H characteristic plus a small-signal linear model relating ΔQ and ΔH to vibration - Eqs. (3), (4) and approximations (16), (17).

Coupling (FSI): substitute the Q, H dependences into the equations of mechanics → obtain coupled equations; analyze them in the frequency domain (to determine amplitudes) and/or solve them numerically in time.

Eq. (15) together with the linear Eqs. (16), (17) provides a simple way to predict the drop in Q/H at a known vibration amplitude; for strong nonlinearities, polynomial (exponential approximations or CFD-based FSI should be used).

When designing dynamic pumps, the geometric parameters of the cross-sectional flow area of the impeller passage are calculated using the numerical value of the

pumped-medium flow rate without considering rotor rotational speed. The numerical value of the circumferential component of flow velocity is used only to calculate the blade installation angle, taking into account the recommended incidence angle. To minimize hydraulic losses, the principle of smooth variation of the translational velocity of the pumped medium is implemented, starting from the initial section of the pump inlet nozzle. The geometry of the inlet flow area across the blade width is calculated taking into account blockage caused by the actual thickness of the blade leading edge, its rounding radius, and the setting angle.

At present, particular attention is paid to current issues such as energy saving and increasing the efficiency of pumping equipment. Energy consumption and environmental safety are indicators of pump unit quality.

The study of the flow of the pumped medium in the pump flow passage using modern computational tools and methods of mathematical modeling has revealed its complex vortex nature [19-22].

Modeling of fluid flow in the blade system was carried out by numerically solving the Navier-Stokes differential equations [23].

To solve the stated problem, it is necessary to identify the energy source causing the vibration, which represents a process of energy dissipation into the surrounding space. As an example, dynamic phenomena in the flow passage of hydraulic machines related to hydrodynamic processes should be considered. The specific types of these machines capable of generating vibration processes with dissipation, that is, with loss of energy, are closely associated with hydraulic energy losses leading to a reduction in the head of pumping units.

Studies show that, in this field, the energy source of vibration of hydrodynamic origin in centrifugal pumps operating at reduced flow is the interaction of the transit fluid flow with the leading edge of the impeller blades, as well as the interaction of different directions of fluid motion within the interblade channels of impellers during hydrodynamic processes [24].

These factors are always present in operating pumps. They are expressed to different degrees depending on the situation. The degree of their manifestation depends on the pump operating mode.

Under the design operating mode of a pump, the fluid flow enters the impeller tangentially to the leading edge of the blades. Achieving this condition is ensured by the appropriate design calculation and structural implementation of this element of the pump flow passage. If the operating mode deviates from the design one, the initial flow velocity field becomes distorted and a mismatch arises between the direction of the relative flow velocity at the impeller inlet tangent to the leading edge (v_1) and the inclination angle of the leading edge α_1 as defined by angle $\alpha_{1\pi}$ (Fig. 1).

As a result, an angle of attack of the flow on the blade is formed, leading not merely to tangential contact between the flow and the blade, but to a force interaction between them. As the pump operating condition (Q), moves away from the design condition (Q_0), the angle of attack i increases and the force interaction between the flow and the blade becomes stronger. With small deviations of the pump operating condition (Q) from the design condition (Q_0), within the pump operating zone, the interaction is slight, but it increases substantially as Q departs from Q_0.

After losing contact with the blade leading edge, the fluid flow enters the interblade channels of the rotating impeller. In this case, the liquid filling the channels is simultaneously forced to exist in several types of motion.

Most of these motions are derivative in nature. Initially, two types of motion are dominant: inertial motion of the liquid in the direction opposite to the impeller rotation, and transit motion under the action of centrifugal force generated by the energy of the pump drive motor.

The forces of these two types of motion, applied to the same mass of liquid, impart a certain resultant motion to the flow. A liquid mass is formed in which regions of disturbance appear and disappear, moving from the inlet of the impeller channels to their outlet. The resulting disturbances impart pulsations to the flow and include unsteady phenomena caused by cavitation processes triggered by separated flow around the confining surfaces, as well as other factors that together create a certain vibroacoustic picture in the pump flow passage. During pump operation within the working zone, the power characteristics are low and can create only a general vibroacoustic background that does not cause significant damage to the equipment. When the pump operating mode leaves the working zone, the situation changes significantly. The vibrations caused by the types of fluid motion considered increase with increasing deviation of the actual mode Q from the design mode Q_0.

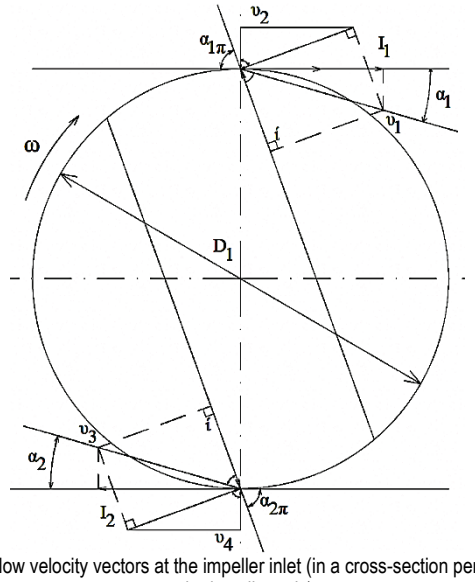


Figure 1 Flow velocity vectors at the impeller inlet (in a cross-section perpendicular to the impeller axis)

Let us consider the interaction between transit and inertial flows using a simplified diagram of fluid motion in the interblade channel of the impeller (Fig. 2).

The liquid located in the interblade channel between blades 1, when the impeller rotates at angular velocity, tends to preserve its state of rest and therefore rotates in the direction opposite to the wheel rotation. The volumes of

liquid located at the wheel outlet are at a greater distance r_2 from the center of rotation than the volumes located near the wheel inlet opening at distance r_1.

The difference in distances leads to the fact that the liquid acquires a higher inertial motion velocity I_2 compared with the liquid at distance r_1, which has velocity I_1.

The difference between I_2 and I_1 causes the liquid filling the interblade channel to rotate relative to the wheel with velocity V_u, directed toward the transit flow entering the interblade channel with velocity V_T after its reflection from the blade leading edge. When the transit and inertial flows meet near the working surface of the blade, their collision leads to force interaction between these flows, which creates the pulsations noted earlier.

When calculating and designing pumps, the interblade channels of the impellers are given geometric shapes intended to ensure favorable interaction between the inertial and transit liquid flows. This can be achieved only within a rather narrow range of flow rates Q. Since the geometric characteristics of the interblade channels become fixed after manufacture, the vector V_u, whose spatial orientation is largely determined by these characteristics, remains almost unchanged and constant. At the same time, the velocity field of the transit flow and, consequently, the orientation of vector V_T changes as the pump operating mode changes. The greater the deviation of Q from Q_0, the greater the mismatch between the transit and inertial flows.

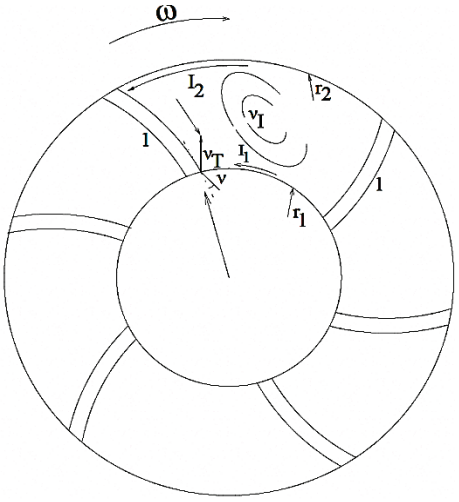


Figure 2 Schematic diagram of the interaction between the transit and inertial flows in the interblade passage of a centrifugal pump impeller

Centrifugal pumps are continuous-flow hydraulic machines operating not periodically, but continuously. The above processes of interaction between the transit flow and the leading edge of the impeller blade and with the inertial flow are continuous. Therefore, they are not accompanied by sufficiently pronounced dynamic impact phenomena that by their nature could cause oscillatory and vibration processes.

According to the studies carried out within this work, the generator of vibration of hydrodynamic origin in the centrifugal pumps under consideration is the tongue of the pump inlet spiral casing (Fig. 3).

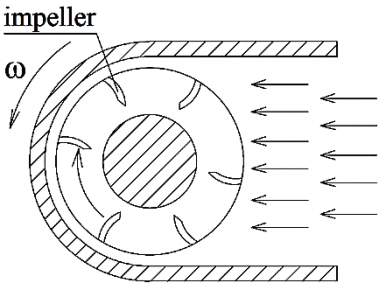


Figure 3 Schematic diagram of fluid flow in the inlet passage of a centrifugal pump with a centrally positioned impeller

The tongue is installed in the inlet spiral casing of the pump directly before the centrifugal wheel inlet to ensure uniform admission of liquid into the interblade channels of the impeller. It fulfills its function by preventing direct entry of liquid into the channels located closer to the pump inlet nozzle, forcing the flow, while moving along the spiral, to fill all the remaining wheel channels sequentially. This provides hydrodynamic balancing of the machine rotor.

During impeller rotation, each channel is alternately blocked by the tongue, which prevents liquid from entering the blocked channel and interrupts the contact of the transit liquid flow entering it with the leading edge of the corresponding impeller blade and with the inertial flow in the blocked interblade channel. After the blocked channel exits the hydrodynamic shadow of the tongue as the wheel continues to rotate, liquid admission into the channel resumes and the transit flow, entering the reopened channel, comes into contact with the blade leading edge and with the inertial flow. In this case, the renewed contact is dynamic and impact in nature. The force of impact between the transit flow and the obstacles in front of it, in the form of the leading edge and the inertial flow, becomes greater as the mismatch between the velocity fields of these flows and the velocity field of the transit flow with the geometric characteristics of the blade leading edge increases. As noted above, this mismatch is almost zero at $Q = Q_0$ and is quite low when Q is within the pump operating zone, but it increases significantly as Q moves away from the boundary of the machine operating zone.

When the transit flow comes into force contact with the leading edge of the impeller blade, the reaction force acts on the blade and, through it, on the impeller and on the pump rotor as a whole. The resulting force is directed normal to the machine rotor axis if the blades are not inclined relative to the impeller discs. When the blades are inclined relative to the wheel discs, impact with the blade generates transverse and axial forces acting on the pump rotor.

Impact between the transit and inertial flows occurs in a liquid medium. The force generated in this case is perceived by the blades and, in addition, by the impeller discs. As a result, the generated transverse and axial forces ultimately act on the pump rotor.

Under the action of these forces, which are periodic in nature, the pump rotor undergoes oscillatory motion. As a result, oscillatory motion is produced throughout the hydraulic machine structure, and the pumping unit enters a vibration regime.

Impact of the transit flow with the leading edges of the impeller blades and with inertial flows in the interblade channels occurs each time access is opened for the transit flow into the next channel opening behind the tongue. This phenomenon occurs at a frequency equal to the number of channels, and therefore blades, in the impeller. If the wheels have a double-sided inlet and matched blades in both halves, then it occurs at a frequency equal to the number of blades in one half of the wheel.

Thus, a physical model of vibration has been developed. According to the proposed physical model of vibration, when centrifugal pumps operate under reduced flow, vibration should be generated in them with frequency φ_Z, for centrifugal pumps operating under reduced flow, equal to the rotational frequency of the machine rotor

$$\varphi_{\text{rot}} = \frac{n}{60} \text{ (rpm)} \tag{24}$$

multiplied by the number of blades in the impeller z, or at the blade-passing frequency

$$\varphi_{\text{rot}} = \frac{n}{60} \cdot z \tag{25}$$

where n – is the pump rotor rotational speed, (1/min).

The angle of inclination of the blades relative to the impeller discs φ may be 0° or, in the case of blades inclined to the discs, of the corresponding order 10° - 20°. With such a wheel design, the force vector arising from interaction of the transit flow with the impeller blades (Fig. 4).

Flow is directed either normal to the pump rotor axis or at some small angle to it. This creates vibration. In the first case, only in the transverse direction; in the second, in both the transverse and axial directions, with the transverse direction predominating.

The main and covering, or front, impeller discs are either equal in diameter or differ only slightly, except in special pump impeller designs. The inner-facing surfaces of these discs likewise have either equal areas or areas that differ only slightly. These surfaces perceive all hydrodynamic consequences of the impact contact of the transit flow with the blade leading edges and with the inertial flow. The consequences of these contacts are pressure pulsations acting on nearly equal-area disc surfaces facing in opposite directions. The resulting forces applied to the discs are nearly equal, act in opposite directions, and mutually compensate each other.

Therefore, in centrifugal pumps operating under reduced flow, according to the proposed model, hydrodynamic vibration should be observed predominantly in the transverse direction; the axial component should also be recorded, but on a smaller scale, mainly in pumps having wheels with blades inclined relative to their discs.

Vibration also occurs in the vertical direction, i.e., a vertical component, because the vibrating massive pump rotor is supported by the machine bearing assemblies. The appearance of the vertical direction is also promoted by the action on the blade that has emerged from the hydrodynamic shadow of the tongue of the pump inlet spiral casing of the above-mentioned pressure pulsations in the corresponding interblade channel of the wheel.

This action is represented by vector v_2 (see Fig. 1).

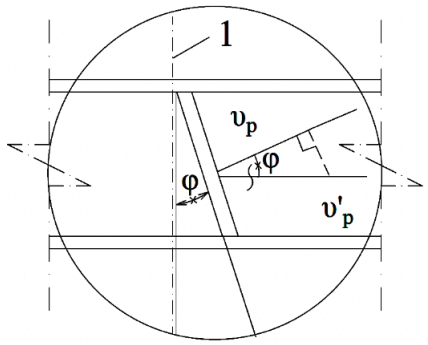


Figure 4 Schematic diagram of the blade positioned between the impeller disks: 1 – direction of the rotation axis of the pump rotor (impeller)

The results of numerous experimental data obtained in vibration tests of pump units confirm the conclusions made above regarding the expected values of vibration parameters in the case considered. As an example, some data from vibration tests of NM-type trunk oil pipeline pumps with a nominal flow rate of 12500 m^3/h. are presented. These pumps have impellers with blades inclined relative to the wheel discs. The number of blades is $Z = 7$. The rotor speed of the pumps is $n = 3000$ rpm.

Table 1 Results of pump vibration tests

Number of the pump	Pump operating mode				Vibration in different directions, 10^{-3} m/s			Vibration frequency, Hz
	Pressure		Head, m	Flow rate Q, m^3/h	Vertical	Transverse	Axial	
	Inlet, MPa	Outlet, MPa						
1	0.98	3.12	258	9700	4.12	13.5	12.7	350
2	0.98	3.14	260	9600	4.2	12.2	11.3	350
3	0.98	3.16	263	9500	4.31	11.6	10.1	350
4	0.98	3.18	265	9250	4.4	10.45	9.18	350
5	0.98	3.20	266	9025	4.55	9.37	7.76	350
6	0.98	3.22	269	8880	4.8	8.3	6.12	350

Tab. 1 presents the results of pump vibration tests under different operating conditions. As the outlet pressure and head increase from 3.12 to 3.22 MPa and from 258 to 269 m, respectively, the flow rate gradually decreases from 9700 to 8880 m³/h. The vibration response is direction-dependent: vertical vibration increases slightly from 4.12 to 4.80 × 10^{-3} m/s, whereas transverse and axial vibrations decrease significantly, from 13.5 to 8.3 × 10^{-3} m/s and from 12.7 to 6.12 × 10^{-3} m/s, respectively. The vibration frequency remains constant at 350 Hz throughout all operating modes.

Based on the above table, we plot graphs of head and flow rate as functions of vibration in the Vertical, Transverse, and Axial directions:

Formula for the vertical line at the optimum: $x_0 = 4.12$ mm/s and $H_{\max} = 269$: $H = -30(x - 4.12)^2 + 269$

Formula for the transverse line at the optimum: $x_0 = 6.12$ mm/s and $H_{max} = 269$: $H = -0.4(x - 6.12)^2 + 269$

Formula for the axial line at the optimum: $x_0 = 8.3$ mm/s and $H_{max}=269$: $H = -0.3(x - 8.3)^2 + 269$

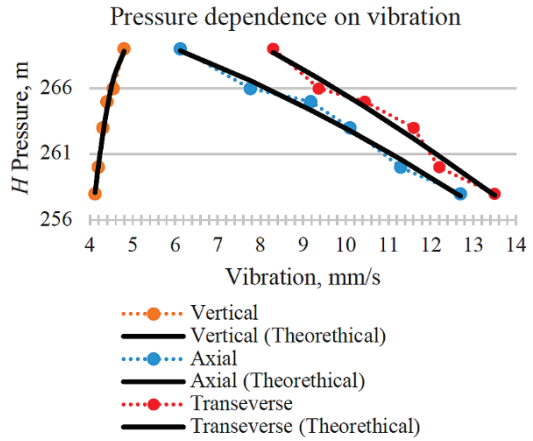


Figure 5 Dependence of pressure *H* on vibration

Formula for the vertical line at the optimum: $x_0 = 4.12$ mm/s and $Q_{max} = 9700$: $Q = -1800(x - 4.12)^2 + 9700$

Formula for the transverse line at the optimum: $x_0 = 6.12$ mm/s and $Q_{max} = 9700$: $Q = -35(x - 6.12)^2 + 9700$

Formula for the axial line at the optimum: $x_0 = 8.3$ mm/s and $Q_{max} = 9700$: $Q = -25(x - 8.3)^2 + 9700$

The plotted graphs show that in all three vibration directions (vertical, transverse, and axial) one main pattern is observed: the higher the head and flow rate, the higher the vibration in all directions. As the head and flow rate decrease, the vibration also decreases. This is due to the fact that, when the pump operates closer to the maximum of the characteristic curve, the following increase: hydrodynamic forces on the impeller and blades, turbulence, axial and radial loads, cavitation micropulsations and vibration of the shaft and supports.

Within the head interval of 258 - 269 m, vertical vibrations as a function of head increase almost linearly from 4.12 - 4.8 mm/s. This small increase indicates uniform distribution of axial forces and good rotor balancing.

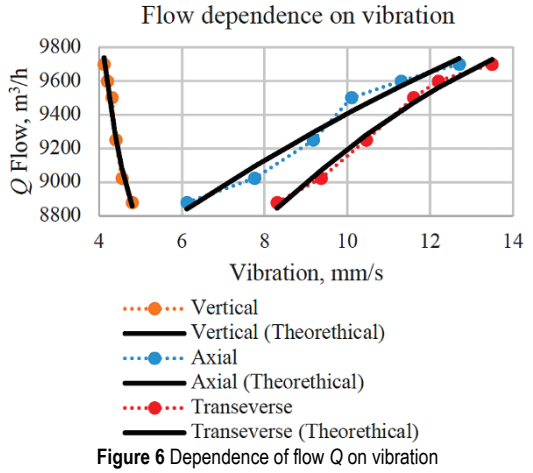


Figure 6 Dependence of flow Q on vibration

Thus, vertical vibration is the most stable and least sensitive to changes in operating conditions. In the transverse direction, vibration decreases from 13.5 - 8.3 mm/s. This is because, as head increases, the pump moves away from the zone of hydraulic instability; that is, in the region of maximum flow the flow becomes more stabilized and the lateral (radial) forces on the shaft decrease. Thus, transverse vibration is the most sensitive parameter indicating the hydraulic stability of the operating mode. In the axial direction, vibration decreases sharply from 12.7 - 6.12 mm/s. This is explained by the fact that, as head increases, the shaft operates closer to its optimum position, axial flow imbalance decreases, and pressure pulsation is reduced. Axial vibration decreases most strongly, which is a sign that the pump is operating closer to the optimum mode in terms of axial forces.

The graphs also show the dependence of vibration on head. In this relationship, the head varies within 258-269 m. The graph shows that vertical vibration grows almost linearly, from 4.12-4.8 mm/s. This slight increase means a uniform distribution of axial forces and good rotor balancing. Vertical vibration is the most stable and least sensitive to changes in operating conditions. Transverse vibration decreases from 13.5-8.3 mm/s. This is because, as head increases, the pump leaves the zone of hydraulic instability; that is, in the region of maximum flow the flow becomes more stabilized and the lateral (radial) forces on the shaft decrease. Transverse vibration is the most sensitive parameter indicating the hydraulic stability of the regime.

The dependence of vibration on flow rate shows that as the flow rate decreases from 9700 to 8880 m³/h, vertical vibration increases, while transverse and axial vibration decrease. The reason is high flow rate, low head, and unstable hydraulics. All this leads to increased turbulence and lateral forces, as well as to flow non-uniformity. Therefore, at high flow rates, transverse and axial vibrations are maximal. As the flow rate decreases, the pump operates closer to its optimum head regime, and therefore vibrations in these two directions fall. The interpretation by direction is given in Tab. 2.

Table 2 Interpretation by direction

Vibration direction	Trend	Reason
Vertical	Slightly increases with increasing head	Increase in the overall load on the bearing
Transverse	Noticeably decreases	The flow becomes more stable, resulting in lower radial forces
Axial	Decreases sharply	Optimization of axial forces and reduction of reverse thrust

Tab. 2 shows that vibration behavior varies depending on the direction of measurement as the pump head increases. Vertical vibration exhibits a slight increase due to the higher load acting on the bearings. In contrast, transverse vibration decreases noticeably because the flow becomes more stable, reducing radial forces. The most significant reduction is observed in the axial direction, which is associated with the optimization of axial forces and the mitigation of reverse thrust.

3 DISCUSSION

Pump operation at high head and lower flow rate reduces transverse and axial vibration and ensures a more stable flow. At high flow rate and low head, however, radial and axial pulsations increase, vibration grows, and stability decreases. NM-type oil pipeline pumps are significantly underloaded in terms of flow at a design capacity of 12500 m^3/h, they operate at 8600 - 9600 m^3/h, and at the same time experience increased vibration. The vibration is evidently hydrodynamic in nature. As noted earlier, the pumping units had no remarks concerning the mechanical part. The recorded vibration exceeds the normal level for this type of machine, characterized by a vibration velocity of 7.1×10^{-3} m/s and occurs at a frequency equal to the blade-passing frequency of the pumps. The same vibration frequency is obtained by calculating it according to the model under consideration, using Eq. (25):

$$\varphi_z = \frac{n}{60}\cdot z = \frac{3000}{60}\cdot 7 = 350 \text{ , Hz} \tag{26}$$

The vibration levels obtained in the three directions show that oscillations predominate in the transverse and axial directions, with the transverse direction prevailing. Vibration is also recorded in the vertical direction, but to a lesser extent compared with the transverse and axial directions.

The results obtained reflect the hydrodynamic processes occurring in pumps with specific design features, containing before the impeller inlet a structural element that fully or partially blocks the entrance to the interblade channels of the wheel. The tongue of the pump inlet spiral casing is characteristic of pumps equipped with double-entry impellers and with the impeller located in the middle of the shaft of hydrodynamic machines; this is one of the most common types of centrifugal pumps. These include main oil pipeline pumps (NM).

A similar element is present in some overhung-type pumps. It is made in the form of a rib along the inner generatrix of the pump inlet nozzle, which simultaneously performs the function of the machine inlet. Its purpose is to prevent or reduce flow swirl before the flow enters the impeller.

4 CONCLUSIONS

1) Testing confirms the expediency of changing the traditional approach to designing the flow passage of the pump impeller and significantly reducing the flow area of its passage section.
2) Increasing the efficiency of a dynamic pump is achieved by minimizing hydraulic losses through optimization of the impeller flow passage.
3) At reduced flow and underloading of centrifugal pumps, increased vibration of hydrodynamic origin arises at a frequency equal to the blade-passing frequency and is recorded in the transverse, axial, and vertical directions. In this case, the predominant oscillations occur in the transverse direction.
4) The presented numerical model adequately reflects the phenomenon under study and explains the nature of the occurrence of the vibration type considered, reveals its specific energy sources and the factors generating the oscillatory motion itself, and explains its distribution along the spatial coordinates.
5) To develop practical recommendations for optimizing the geometry of the impeller flow passage, additional computational and experimental studies are required.
6) Hydrodynamics can modify natural frequencies and damping, creating a resonance risk.
7) The main reason for the strong sensitivity of Q/H to vibration is the presence of resonances and nonzero hydraulic sensitivity to displacements.
8) If the natural frequencies of the mechanics intersect with the operating frequencies, it is necessary to change stiffness/damping or choose another operating mode (for example, according to Pontryagin).

Acronyms

CFD	Computational Fluid Dynamics
FSI	Fluid-Structure Interaction
ODE	Ordinary Differential Equation
ESP	Electric Submersible Pump
NM	Type of mainline oil pipeline pumps
MPC	Model Predictive Control

Acknowledgements

The author(s) special thanks go to the staff of the Scientific-Research Institute "Geotechnological Problems of Oil, Gas and Chemistry", Baku, Azerbaijan for providing useful suggestions.

5 REFERENCES

[1] Chugaev, R. R. (2014). *Hydraulics, hydraulic machines and hydraulic drives*. Mashinostroenie.
[2] Stepanov, A. J. (1993). *Centrifugal and axial flow pumps: Theory, design and application*. Wiley.
[3] Gülich, J. F. (2010). *Centrifugal pumps*. Springer. https://doi.org/10.1007/978-3-642-12824-0
[4] Lebedev, A. A. (2015). *Vibrations in engineering and technologies*. Mashinostroenie.
[5] Ehrich, F. (1999). *Handbook of rotordynamics*. McGraw-Hill.
[6] Rao, J. S. (2011). *Rotor dynamics*. New Age International. https://doi.org/10.1007/978-94-007-1165-5_14
[7] Tymchak, V. S. (2008). *Dynamics and vibrations of rotor machines*. Tekhnika.
[8] Tokarev, M. P. (1983). *Transient processes in hydraulic systems*. Mashinostroenie.
[9] Babakov, A. M. (2000). *Hydraulics of oil pumping systems*. Nedra.
[10] Zheverev, S. V. (2012). *Theory of centrifugal pumps*. Politekhnika.
[11] Monin, A. S., & Yaglom, A. M. (2000). *Statistical hydromechanics*. Nauka.

[12] Nayfeh, A. H., & Mook, D. T. (1995). *Nonlinear oscillations*. Wiley. https://doi.org/10.1002/9783527617586
[13] Basarygin, Yu. M., & Vlasov, A. L. (2015). *Dynamics of ESP operation*.
[14] American Petroleum Institute. (2020). *API RP 11S5: Recommended practice for ESP system vibration*. API.
[15] Martyanov, A. V. (2017). *ESP: Theory and practice of operation*. TyumGNIIPI.
[16] Schlumberger. (2016). *ESP design manual*. Schlumberger.
[17] Baker Hughes. (2018). *ESP system reliability and vibration analysis*. BHGE.
[18] Ogata, K. (2010). *Modern control engineering*. Prentice Hall.
[19] Kochevsky, A. N., & Nenya, V. G. (2014). *Modern approach to modeling and calculation of fluid flow in blade hydraulic machines*.
[20] Sokolov, E. V., & Ankudinov, D. T. (2007). Numerical simulation of working processes in centrifugal pumps as a method for improving their efficiency. *Lesnoy Vestnik, 11*(8), 165–169.
[21] Slobodkina, F. A., Malinin, A. V., Malinin, V. V., & Shigapova, D. Yu. (2008). Fluid flow in a centrifugal pump stage. *Mathematical Modeling, 20*(10), 51–62.
[22] Borovsky, B. I. (1989). *Energy parameters and characteristics of high-speed blade pumps*. Mashinostroenie.
[23] Anderson, D., Tannehill, J., & Pletcher, R. (1990). *Computational fluid dynamics and heat transfer*. Mir.
[24] Sokolov, E. V., & Ankudinov, D. T. (2006, September 20–21). Modeling of fluid flow in centrifugal pumps. In *Proceedings of the Eurasian Symposium "Wood Processing: Technologies, Equipment, Management of the XXI Century"* (pp. 217–221). Ural State Forest Engineering University.

Authors' contacts:

Amir G. Mustafayev, Associate Professor
Faculty of Mechanical Engineering,
Azerbaijan State Oil and Industry University,
Azadliq avenue 43, AZ 1118 Baku, Azerbaijan
mustafaev-1959@mail.ru

Sanam J. Muslimov, PhD Researcher
(Corresponding author)
Department of Industrial Machines,
Scientific-Research Institute "Geotechnological Problems of Oil, Gas and Chemistry",
Azadliq avenue 43, AZ 1118 Baku, Azerbaijan
sanammuslimov@gmail.com